ROYAL SOCIETY OF CHEMISTRY

PAPER

Check for updates

Valorisation of invasive plant (*Rhododendron ponticum*) biomass into activated biochar as a sustainable adsorbent for emerging pharmaceutical contaminant removal from water

Tielidy A. de M. de Lima, [ID] *[ab] Matheus S. T. Arantes,[c] Jeovan A. Araújo, [ID] [b] Gabriel G. de Lima,[bd] Dayanne R. M. Andrade,[c] Emma J. Murphy,[ab] Washington L. E. Magalhães [ID] [c] and Michael J. D. Nugent*[b]

The common issue of water contamination by pharmaceuticals are increasingly recognised as emerging contaminants in water as they pose significant environmental and health risks, necessitating innovative and sustainable approaches to water treatment. Activated biochar represents an effective solution for the removal of pharmaceuticals from water. Here, the focus was on the valorisation of *Rhododendron ponticum*, an invasive plant species in Ireland, into high-surface-area activated biochar through thermo-chemical treatments. In this work, phosphoric acid (H_3PO_4) was used for activation at two different temperatures (550 and 650 °C), which resulted in activated biochars that exhibited excellent adsorption properties with surface area of 876.3 and 869.2 m^2 g^{-1} when treated at 550 and 650 °C, respectively. Structural and composition properties of the produced biochars were investigated by elemental CHNS (carbon, hydrogen, nitrogen, and sulphur) composition analysis, moisture content, fixed carbon, ash, and volatile matter. Acetylsalicylic acid (ASA), commonly referred to as aspirin, was used as a model pharmaceutical compound, and its removal from water was significantly enhanced by the activation process. The inactivated biochar showed the lowest ASA adsorption (113 mg g^{-1}), whereas the activated biochar exhibited much higher adsorption levels (267–296 mg g^{-1}). These results demonstrate that the biochar produced here is highly effective for the removal of aspirin from water. By converting problematic invasive biomass into a valuable resource, this work contributes to addressing environmental concerns associated with both invasive species and water pollution by developing eco-friendly adsorbent materials for removing emerging pharmaceutical contaminants from water.

Sustainability spotlight

This article demonstrates a circular and sustainable approach to valorise invasive *Rhododendron ponticum* biomass into high-performance activated biochar, which was activated by mechanochemical and thermochemical treatments in a tandem approach. As a demonstrative application, the sustainable activated biochar materials were used as adsorbents for the removal of aspirin—a model emerging pharmaceutical contaminant in water. Our approach illustrates how waste biomass can be valorised into functional materials, offering scalable opportunities to adapt this method to other invasive feedstocks worldwide, and it advances low-cost, eco-friendly solutions for cleaner water. This work contributes to ecosystem restoration, resource efficiency, and public health protection, aligning with UN Sustainable Development Goals 6 (Clean Water and Sanitation), 12 (Responsible Consumption and Production), and 15 (Life on Land).

Introduction

Pharmaceuticals removal from contaminated sources and effluents in the environment has sparked significant interest in the search for effective wastewater treatment methods, given their toxicity, persistence, and resistance to biodegradation.[1] Adsorption of pharmaceutical pollutants onto activated carbonaceous materials emerges as a promising approach due to its proven efficiency and wide applicability. Conventional treatment technologies such as coagulation–flocculation, biological treatment, and chlorination are often ineffective in removing

[a]Bioengineering Organ-on-Chip Research Group, Centre for Applied Bioscience Research, Technological University of the Shannon: Midlands Midwest, V94 EC5T Limerick, Ireland. E-mail: Tielidy.lima@tus.ie

[b]PRISM Research Institute, Technological University of the Shannon: Midlands Midwest, N37 HD68 Athlone, Ireland. E-mail: Michael.Nugent@tus.ie

[c]Embrapa, Estrada da Ribeira, Km 111, CEP: 83411-000 - Colombo, Parana, Brazil

[d]Research Center for Rheology and Non-Newtonian Fluids-CERNN, Federal University of Technology-Parana-UTFPR, Dep. Heitor Alencar Furtado, 5000 – Bloco N – Ecoville, Curitiba, PR, 81280-340, Brazil

pharmaceutical pollutants. However, adsorption alone merely transfers pollutants between phases without degrading them, highlighting the potential of combining adsorption with advanced oxidation processes or other catalytic degradation methods. Recent advances in materials science, such as metal–organic frameworks (MOFs), demonstrate that dual-function adsorbent-catalyst systems can enhance pharmaceutical removal by simultaneously adsorbing and degrading pollutants.[2] In this context, adsorption onto activated carbonaceous materials, particularly biochar, stands out as a promising, sustainable, and cost-effective solution, offering high surface area, porosity, and catalytic potential for environmental applications.[3]

The use of biomass for biochar production, in addition to contributing to water decontamination, offers additional benefits such as reducing organic waste and promoting sustainability. By harnessing renewable organic materials, such as agricultural crop residues or forest waste, for biochar production, it is possible to mitigate water contamination and promote more sustainable, eco-friendly practices. *Rhododendron ponticum* (*R. ponticum*), an invasive species found across various regions of the world, has been the focus of control efforts due to its negative impact on local ecosystems. This invasive shrub is considered an environmental threat to Atlantic forests in continental Europe,[4] particularly in areas such as western France[5] and the British Isles.[6] In the Republic of Ireland, for instance, the government has made significant financial investments in its removal from Connemara National Park. Nonetheless, the resulting biomass from this species presents a valuable opportunity for the production of useful materials, such as activated biochar, through renewable biomass valorisation methods.

To chemically activate biochar, various chemical treatment options are available. Treatments include acids such as: phosphoric acid (H_3PO_4) and sulfuric acid (H_2SO_4),[7–9] or bases like potassium hydroxide (KOH) and sodium hydroxide (NaOH),[10,11] and salts such as metal chlorides including zinc or potassium chloride,[12,13] among other methods. In this context, this work focuses on H_3PO_4, which is one of the most commonly employed agents for the chemical activation of biochar. The process involves mixing H_3PO_4 with biochar and subjecting it to heat, resulting in increased porosity. Studies have highlighted that different biochar modification strategies, such as acid–base treatments and metal impregnation, significantly increase its surface area, the availability of functional groups, and, consequently, its efficiency in removing organic and pharmaceutical pollutants.[14,15]

So far, only one study in the literature has produced activated carbon from *R. ponticum* L.[16] produced activated carbon *via* physical and chemical activation, aiming at measuring the adsorption of iodine. At 550 °C, the carbon achieved the highest Brunauer–Emmett–Teller (BET) surface area (1470 m² g⁻¹) and microporous surface area values (1383 m² g⁻¹). With these parameters, the authors produced the optimal activated carbon using KOH with a surface area of 1199 m² g⁻¹, whereas H_3PO_4 had 124 m² g⁻¹ and K_2CO_3 presented the lowest 60 m² g⁻¹.[17]

This indicated that the treatment used can significantly alter the characteristics of adsorption.

Another alternative for producing activated carbon is the utilization of mechanochemical pre-treatment. This approach has emerged as a promising method to enhance the efficiency and quality of the produced biochar. Such as the work from Tayibi *et al.*,[18] in which the authors produced an activated biochar from Moroccan algae residue mixed with olive pomace using mechanochemical activation using NaOH and ball milling (BM). The activated biochar produced using BM had the highest ζ-potential value (−59.7 mV), and demonstrated superior methylene blue removal efficiency compared to other activated biochar without grinding.

In alignment with current developments reported in the literature, this study focusses on evaluating the adsorption capacity of pharmaceuticals using activated biochar valorised from biomass waste. The objective is to produce and assess the feasibility of using activated carbon derived from *R. ponticum* residues for the removal of pharmaceutical compounds from aqueous solutions. A combined mechanochemical pre-treatment was employed, involving BM and chemical activation with H_3PO_4, followed by a series of washing steps to enhance the physicochemical properties of the resulting biochars.

Aspirin, one of the earliest and most widely used pharmaceutical compounds for the treatment of pain, fever, and inflammation, has been frequently detected in aquatic environments across various regions.[19,20] Due to its widespread use, environmental prevalence, and physicochemical properties that make it representative of other emerging pollutants, aspirin has been studied as a model pharmaceutical contaminant in this study. Notably, aspirin is produced and consumed globally at a scale of approximately 35 000 tonnes per year, leading to its continuous release into the environment and detection in surface, ground, and even drinking waters.[21] Moreover, persistent release of aspirin into water bodies raises concerns regarding bioaccumulation in aquatic microorganisms, which may subsequently transfer through the food chain and pose potential risks to human and ecosystem health, thereby emphasizing the need for effective and sustainable removal strategies. Studies also highlight that conventional wastewater treatment plants are not specifically designed to eliminate such refractory pharmaceutical compounds, contributing to their persistence in the environment.[21]

Studies have demonstrated that conventional wastewater treatment plants are frequently ineffective at fully removing pharmaceutical residues, particularly non-steroidal anti-inflammatory drugs (NSAIDs) such as aspirin, resulting in their recurring detection in drinking water sources across various countries, including India, Germany, Spain, and Poland. This persistent contamination increases the toxicological impact on water systems, raising serious concerns about public health and highlighting the urgent need for reliable detection and monitoring strategies.[22] Herein, we propose to use aspirin as a model pollutant to enable the assessment of the prepared activated biochar in terms of its capacity to adsorb pharmaceuticals under realistic environmental conditions, and

to ultimately support the development of bio-based treatment technologies targeting a broad class of emerging contaminants.

Invasive *R. ponticum* biomass can be valorised into high-performance activated biochar through a combined mechano-chemical pre-treatment and phosphoric acid activation. This dual approach is expected to significantly enhance the physi-cochemical properties of the resulting biochar, surface area, porosity, and functional group density, thereby improving its adsorption capacity for pharmaceutical pollutants. Using aspirin as a model contaminant, the activated biochar is anticipated to demonstrate superior removal efficiency compared to its non-activated counterpart, validating its potential as a sustainable, low-cost adsorbent. Beyond pollutant removal, this strategy provides a dual environmental benefit: mitigating the ecological burden of an invasive species while contributing to sustainable water treatment solutions.

Experimental section

Materials

Branches of the invasive *R. ponticum* scrub were originally collected from Connemara National Park (county Galway, Ireland), and kindly provided by the Atlantic Technological University, Galway campus. Initially, the biomass was grinded into sawdust using a mill by Marconi (Piracicaba, SP, Brazil). H_3PO_4 and hydrochloric acid (HCl) were purchased from Merck Brazil (Curitiba, PR, Brazil).

Preparation of invasive plant waste-derived activated biochar

Pyrolysis of *R. ponticum* waste biomass. Previously milled waste biomass derived from *R. ponticum* was initially pyrolyzed, according to a modified procedure adapted from Sütcü,[17] which was then valorised into high-surface-area activated biochar through tandem mechanochemical ball-milling and thermo-

chemical acidic activation treatments, as depicted in Fig. 1. Firstly, the pyrolysis of *R. ponticum* sawdust was performed in a Jung muffle furnace (Blumenau, SC, Brazil), heated at 5 °C min^{-1} in a close low-oxygen atmosphere and maintained at 550 °C for 2 h.

Ball-milling. 100 g of the pyrolyzed biomass sample was ball-milled rotating for 12 h to obtain the biochar. The biochar samples were milled using a low-energy ball mill from Servitech (Chiarotti-type) equipped with ceramic grinding bowls. The milling was carried out at a rotation speed of 40 rpm. Approximately 10 g of biochar was placed in the bowl along with 200 g of ceramic balls (∅ 10 mm), maintaining a ball-to-sample mass ratio of about 20 : 1. The jar was filled to around 50% of its total volume, with ∼30% occupied by the sample and ∼20% by the ceramic balls, in accordance with standard milling practice for this type of equipment.

Chemical activation. The resulting ball-milled biochar was treated with a 50% H_3PO_4 aqueous solutions. The mass ratio of the acid solution to biochar was 2 : 1 which was thoroughly mixed with the activating agent solution for 15 minutes. Subsequently, this mixture underwent drying in an oven for 24 h at 103 ± 2 °C. Following the drying step, activation occurred in a muffle furnace at two different temperatures: 550 and 650 °C. The heating rate during activation was set at 10 °C min^{-1}, and the activation duration was 1 h for each temperature. The resulting material was subjected to washing with hot deionized (DI) water, followed by rinsing with a solution containing 10% HCl, and finally washed again with DI water until the conductivity of the washing water dropped below 40 μS cm^{-1}. The activated carbon was then dried in an oven at 103 ± 2 °C until it reached a constant mass. The specimens were designated as biochar (BC) at two different activation temperatures, namely ABC550 and ABC650 (Fig. 1).
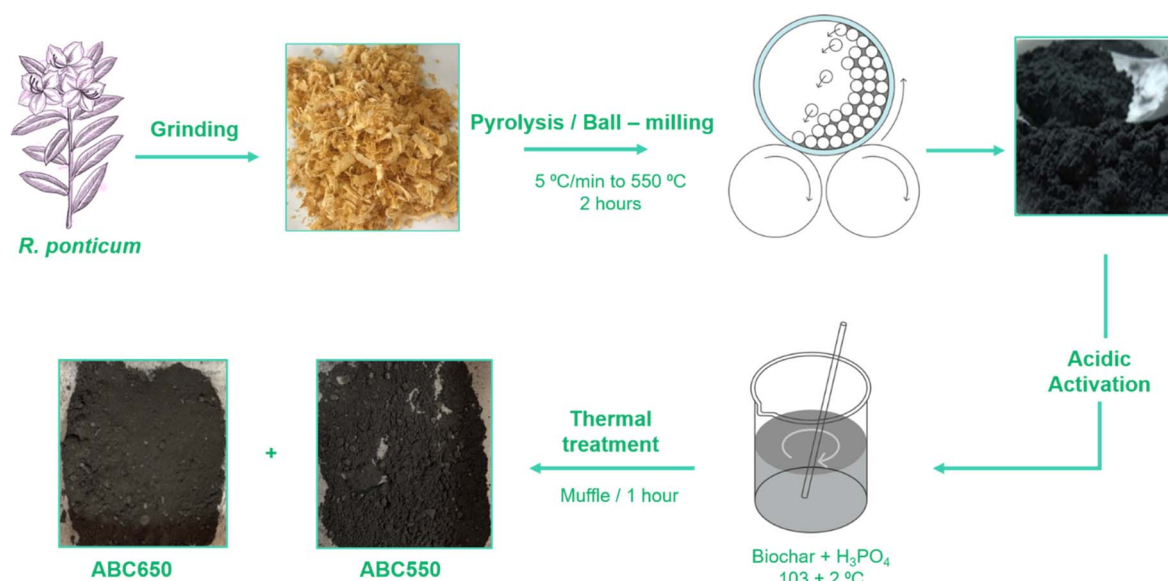

Fig. 1 Illustration of the sustainable approach used to valorise invasive *R. ponticum* waste biomass into high-surface area activated biochar by combining mechanochemical ball-milling and thermo-chemical acidic activation. Two activated biochar samples ABC550 and ABC650 were obtained after thermal treatments at 550 and 650 °C, respectively.

Characterisation. The FTIR analysis was performed using the Nicolet™ iN10 MX Infrared Imaging Microscope from Thermo Scientific. The IR spectra were recorded in the spectral range of 4000–600 cm^{-1}, utilizing 16 scans per sample. Conductivity measurement was conducted using a conductivity meter, DI-GIMED DM-32. The measurements were taken on the liquid after washing using 1 L of DI water, followed by rinsing with a 1 L solution containing 10% HCl, and finally washing again with DI water until the conductivity of the washing water dropped below 40 μS cm^{-1}. A sample was taken for each Liter used in washing to measure BET and conductivity. The intention of this study is to establish a correlation between the surface area and the conductivity of the liquid at each wash. These values can be found in Fig. 2.

The surface area was determined employing the Brunauer–Emmett–Teller (S$_{BET}$) technique.[23] Prior to measurement, the biochar underwent degassing at 300 °C under vacuum for 3 h. Subsequently, the specific surface area and pore structure features of the biochar were assessed through nitrogen adsorption/desorption at −196 °C using a surface area analyser from Quantachrome Instruments, NOVA 1200e (Boynton Beach, FL, USA).

The elementary analysis of the activated carbon, including calorimetry, CHNS (carbon, hydrogen, nitrogen, and sulphur), ash, and volatiles, was conducted for material characterisation. A Mira scanning electron microscope (SEM) from Tescan Orsay Holding (Brno, Czech Republic) was utilized to examine the structure of biochar and ABC550 and ABC650 in back-scattered electron (BSE) mode. Prior to imaging, the specimens underwent gold coating using a Baltec SCD 005 sputtering device for approximately 110 seconds under a vacuum of 0.1 mbar, resulting in a coating thickness of approximately 110 nm. Images were captured at an acceleration voltage of 20 kV, with a magnification of 1000x.

The biochar sample BC, ABC550 and the ABC650, weighing approximately 4–5 mg each, were encapsulated in standard aluminium pans to record the first derivative thermogravimetry (DTG) curves. Thermograms were recorded at a rate of 10 °C min^{-1} within a temperature range of 20–1000 °C, using an empty aluminium pan as the reference. These experiments were conducted under a nitrogen flow of 50 mL min^{-1} using a Q600 SDT—TA Instruments (TA Instruments, New Castle, PA, USA). A Siemens D500 X-rays powder diffractometer (Karlsruhe, Germany) with Cu Kα radiation ($\lambda = 0.15418$ nm) was used to obtained the diffractograms. Diffraction patterns of the biochar samples before and after chemical activation (ABC550 and ABC650) were obtained in the range of $2\theta = 10$–50°, operating at a voltage of 40 kV, a current of 7.5 mA, and a step size of 20°.

Adsorption analysis. Sorption efficiency of the three developed materials was evaluated considering the removal of Acetylsalicylic Acid (ASA). Adsorption isotherms were obtained in triplicate with 50 mg of adsorbent and 50 mL of ASA solution (C_o = 50–800 mg ASA L^{-1}). The mixture was kept in an incubator with controlled temperature and agitation (25 ± 2 °C, 100 rpm, 24 h), and it was filtered with a filter paper. The UV-Vis spectrophotometric analyses were performed using UV-Vis Spectrophotometer Shimadzu 1800. ASA showed a characteristic absorption peak at 276 nm. A calibration curve was constructed in the working concentration range (4.9–204 mg L^{-1}), showing an excellent linear fit with the equation $C = 157.20 \times \text{Abs} + 3.77$ and coefficient of determination $R^2 = 0.9993$, in compliance with the Beer–Lambert law. Dilutions were applied when necessary to keep the absorbance values within the linear range, and the adsorbed amount and the removal efficiency were calculated according to eqn (1) and (2), respectively.

$$q_{eq} = \frac{(C_o - C_{eq}) \times V}{w} \quad (1)$$

$$\text{RE} = 100 \times \frac{C_o - C_{eq}}{C_o} \quad (2)$$

where q_{eq} (mg ASA g^{-1} adsorbent) is the equilibrium adsorbed amount, C_o and C_{eq} (mg ASA L^{-1}) are the initial and equilibrium concentration of ASA in the liquid phase, V (0.050 L) is the volume of solution used in the adsorption experiment, w (g) is the weight of adsorbent, and RE (%) is the removal efficiency.

Adsorption isotherm analysis. Isotherm studies were conducted using BC, ABC550, and ABC650. The experimental data was analysed by fitting two conventional isotherm models, the Langmuir (eqn (3)) and Freundlich (eqn (4)) isotherm models,[24] using the equations provided below:

$$q_{eq} = \frac{q_L k_L C_{eq}}{1 + k_L C_{eq}} \quad (3)$$

$$q_{eq} = k_F c_{eq}^{\frac{1}{n}} \quad (4)$$

Where q_L (mg ASA g^{-1} adsorbent) and k_L (L mg^{-1} ASA) are the Langmuir isotherm parameters, and n and k_F (mg$^{(1-1/n)}$ ASA L$^{1/n}$ g^{-1} adsorbent) are the Freundlich isotherm parameters.
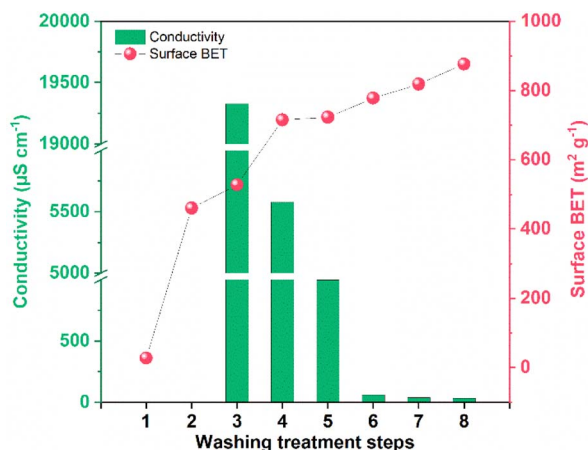

Fig. 2 Measurements of solution conductivity and BET surface area of the ABC550 sample after several washing treatment steps (step 1: hot DI water; step 2: HCl solution; and steps 3–8: DI water at room temperature). Conductivity axis was intentionally omitted from 1000–5000 and 6000–19000 μS cm^{-1} for clarity and comparison purposes.

Results and discussion

Evaluating biomass potential involves examining diverse factors, including species, compositions, and raw material

characteristics. Crucial among these are physical attributes like moisture content, carbon content, and heating value, which dictate the practical applications of the resulting products. The elemental composition analysis of activated biochar, encompassing moisture content, fixed carbon, ash, and volatile matter, is presented in Table 1. The analysis shows that the properties of activated biochar vary depending on the temperature of activation. Generally, activated biochar produced at higher temperatures (e.g., 650 °C) tends to have lower moisture, volatile matter, and ash content, as well as higher fixed carbon content.[25] Moisture content is crucial as it affects the handling and storage of the material. Lower moisture content generally indicates better stability and shelf life. ABC650 exhibits the lowest levels of both moisture content and volatile matter, measuring at 4.11% and 14.68% respectively. The volatile matter results show a notable decrease from BC (27.82%) to ABC550 (19.03%), and a further decrease for ABC650 (14.68%). This trend suggests that as the activation temperature increases, there is a consistent reduction in volatile matter content. This decrease in volatile matter content can be attributed to the activation process, which involves heating the precursor material to high temperatures in the absence of oxygen. During this process, the phosphoric acidification results in highly volatile organic compounds that are consumed in the pyrolysis, leaving behind a more purified carbon structure which might wide the pore size. The decrease in volatile matter content indicates a higher degree of carbonization and increased carbon purity in the activated biochar samples compared to BC.[26] The ABC650 demonstrates the highest fixed carbon content at 78.0%, the ABC550 69.3% and the BC 63.5%. These results suggest that as the activation temperature increases, the fixed carbon content also increases, likely due to the removal of volatile organic compounds and the rearrangement of carbon atoms, leading to a more ordered structure with higher carbon content, aligning with the conclusions drawn by Liu et al.[27] CHNS results revealed a reduction in carbon content following activation. The values for hydrogen (H), nitrogen (N), and sulphur (S) did not change significantly before and after activation, as evidenced by minimal differences in their measurements.

Gündüz et al.[28] analysed three types of wood pellets (Rhododendron ponticum, Laurus nobilis, and Castane sativa) in terms of ash content and heating values, and how the wood type impacts the pellet quality. Interestingly, R. ponticum provided a higher heating value (20.6 MJ kg⁻¹) and had a lower ash content (1.16%) than the other species studied. These values significantly exhibit the great potential in using this species in the production of activated biochar. In addition, the energy released during combustion can be utilized in various applications, such as for electricity generation in thermal power plants, residential heating, or other industrial applications.[29–31] In this research, branches of R. ponticum were used to produce activated biochar, and the sawdust before carbonization exhibited a heating value of 16.6 MJ kg⁻¹. The samples studied herein were biochar (BC), activated biochar at 550 °C (ABC550) and at 650 °C (ABC650).

For the surface area S_{BET} the results for BC, ABC550 and ABC650 were 491.3, 876.3 and 869.2 m² g⁻¹, respectively. The BC sample showed a surface area of 491.3 m² g⁻¹ before any activation treatment. Biochar naturally possesses a certain level of porosity, which contributes to its surface area.[32] Activation with H_3PO_4 at 550 °C has led to a significant increase in S_{BET} area compared to the untreated BC. This suggests that the activation process at this temperature has been effective in creating additional pores within the biochar structure, resulting in a higher S_{BET} area. Activation with H_3PO_4 at a higher temperature (650 °C) has also resulted in an increase in S_{BET} area compared to the untreated BC. However, the S_{BET} area obtained at 650 °C is slightly lower than that achieved at 550 °C. This could be due to several factors such as changes in the pore structure, pore size distribution, or even partial closure of pores at higher temperatures, leading to pore widening but with a concurrent decrease in surface area. This suggests that the activation process at 550 °C might be more favourable for maximizing the surface area of the studied biochar. Nevertheless, both temperatures have resulted in biochar samples with considerably higher surface areas, which can be advantageous for various applications such as adsorption, filtration, and catalysis. Lower activation temperatures offer advantages such as reduced energy consumption, allowing for cost savings, and may enable better control over porosity, potentially leading to broader pore size distribution advantageous for specific applications. Additionally, lower temperature activation could be more time and resource-efficient. Ultimately, the selection of activation temperature depends on desired product properties and application requirements, but lower temperatures often present favourable outcomes, including energy conservation and enhanced porosity control.

To further investigate the effect of the washing treatment on the adsorbent surface area, washing treatment steps were carried out following the chemical activation of the synthesized BC. The aim of this procedure was to eliminate impurities and unwanted minerals that originate from chemical activation, such as cations and anions from minerals present in the biomass, and phosphoric acid used during the activation step. These compounds are lixiviated into the washing water, resulting in a high electrical conductivity solution. The

Table 1 Proximate (chemical) and ultimate (elemental) composition and BET surface area analysis of the fabricated BC and its respective activated forms

Analysis	BC	ABC550	ABC650
Moisture (wt%)	6.0 ± 0.1	7.3 ± 0.1	4.1 ± 0.3
Volatiles (wt%)	27.8 ± 1.9	19.0 ± 0.8	14.7 ± 2.9
Ash (wt%)	2.6 ± 0.3	4.4 ± 0.3	4.7 ± 0.4
Fixed carbon (wt%)[a]	63.5 ± 1.7	69.3 ± 0.9	78.0 ± 1.1
C (wt%)	80.4	76.6	78.0
H (wt%)	2.8	3.3	3.2
N (wt%)	0.4	0.5	0.4
S (wt%)	—[b]	—[b]	—[b]
S_{BET} (m² g⁻¹)	491.3	876.3	869.2

[a] By difference. [b] Below 0.1 wt% or not detected.

optimization of the water volume used during the washing step is essential, in order to reduce the consumption of water for the development of a greener biochar production process. Fig. 2 presents the measurements of solution conductivity and biochar S_{BET} area through subsequent washing steps.

During the first washing steps, a high concentration of these impurities is observed in the biochar, and their lixiviation to the water is facilitated, resulting in high conductivity of the solution. As the concentration of the impurities on the biochar diminishes, the solution conductivity also diminishes, which is associated to the lower lixiviation chemical potential. Surface area of the biochar after the initial washing steps (1st–5th wash) is observed to increase, which might be associated to the presence of H_3PO_4 molecules present in the surface of the material. Adsorbed H_3PO_4 molecules reduce the number of available active sites in the biochar for the adsorption of other molecules, resulting in a lower N_2 adsorption during the surface area analysis and, consequently, a smaller calculated surface area. After the 5th washing step, however, biochar's surface area is observed to stay stable, with minor oscillations (818.7–876.3 m^2 g^{-1}). Intensifying the washing procedure is essential during the obtention of activated carbon, for it reduces the contamination of the solution with unwanted ions from the biochar and promotes significative difference in the surface area of the material, which is directly associated to its sorbent efficient. Ions in water can influence the adsorption efficiency of biochar due to direct competition for active sites. Inorganic cations such as Na^+, K^+, Ca^{2+}, and Mg^{2+} may compete with target molecules for adsorption, with divalent ions generally having a stronger negative effect because of their higher charge and greater affinity for the adsorbent surface. Anions such as Cl^-, SO_4^{2-}, and NO_3^- can also interfere with electrostatic interactions, reducing removal efficiency. The extent of this interference depends on solution conditions like pH and ionic strength, as higher pH values can modulate electrostatic repulsion depending on the surface charge of the biochar. Despite this, certain adsorbents maintain relatively robust performance even in the presence of competing ions, demonstrating selective adsorption behaviour.[33] For this work, the 8th washing step was assumed as the optimal point, for it resulted in a small variation on the electrical conductivity compared to the previous washing step (34–37.6 μS cm^{-1}) and a small variation on the surface area (876.3–778.6 m^2 g^{-1}). These results suggest that the washing step can be optimized by adopting a conductivity-based stop criterion ($\sim$40 μS cm^{-1}), since most impurities are removed in the first washes. Combined with counter-current reuse of water and recovery of phosphates from the effluent, this strategy reduces water demand and wastewater generation, contributing to a more sustainable process.

Characterisation of the waste biomass-derived adsorbents

The FTIR spectra for BC, ABC550, and ABC650 can be observed in Fig. 3. The peaks identified here for the BCs activated with H_3PO_4 exhibit a similar pattern to that of commercial activated carbon found in the literature.[34] For the activated biochar samples (ABC550 and ABC650) the peak observed at 1546 and
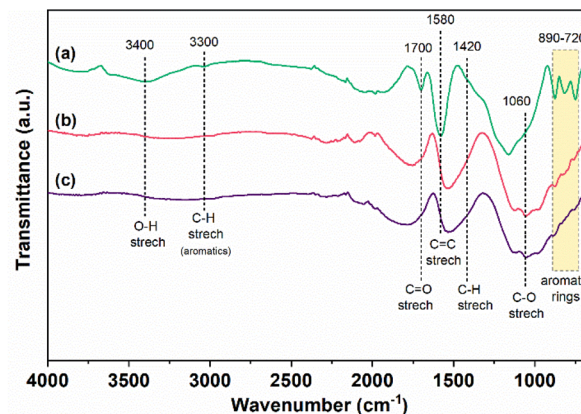

Fig. 3 FTIR spectra of the (a) BC, (b) ABC550, and (c) ABC650 biochar samples. Scans were recorded in the spectral range of 4000–600 cm^{-1}.

1389 cm^{-1} can be attributed to the absorption of energy by the alkyne group (C$\equiv$C) and C–C bond, respectively.[35] FTIR for BC without activation showed peaks in 1576, 1700, 1173, 875 and 740 cm^{-1}. These peaks reflect the molecular composition of the material, including the stretching vibration of aromatic C$=$C bonds (1576 cm^{-1}), carbonyl groups C$=$O (1700 cm^{-1}), stretching vibration of C–O (1060 cm^{-1}) bonds, indicating the presence of ether groups or possibly alcohols in the BC structure (1173 cm^{-1}), and various types of hydrocarbons (875 and 740 cm^{-1}). By correlating the peak intensity with chemical treatment, Barakat et al.[36] found that untreated and H_3PO_4-treated samples exhibit highest intensities, while combined-agent treated samples show lower peaks. This suggests that extensive dissolution of chemical compounds occurs when the combined agent is used in the activation process, potentially contributing to the favourable electrochemical characteristics observed in this sample. After activating the biochar, the temperatures reached is well within the limits for carboxyl decomposition and it may have been the reason for the disappearing peak around 1700 cm^{-1}, and while is being enlarger by a sum of factors, it red-shifts. The broadening increases with temperature, indicating a more diverse range of conformation and, therefore, possibly yielding large number of low molecular weight species in the solid phase as corroborated by Table 1. Additionally, the treatment with H_3PO_4 is known to yield higher carbon at temperatures above 300 °C, thereby explaining the decrease in carbonyl and carboxyl bands. This also is related to the appearance of C–O stretch group. Moreover, the formation of ester at intermediate temperatures is also known to occur using H_3PO_4, also explaining the broadening of the peak due to various ester groups. The aromatic rings region presents to be slightly seen on the activated biochar, the reorganization of carbon into larger, more stable non-aromatic structures, contributes to IR absorption. As a result, the FTIR spectra may no longer show the characteristic peaks of aromatic C$=$C stretching. Finally, H_3PO_4 in biochar treatment acts as a catalyst for bond cleavage and crosslink formation while also creating phosphate linkages between biopolymer fragments. These

linkages can later hydrolyze or oxidize, forming oxidized phosphorus-containing functional groups like $C–O–PO_3$ and $(CO)_2PO_2$.[37]

X-ray diffraction (XRD) analysis presented in Fig. 4a shows crystalline structure and amorphous phase for BC, AC550 and AC650. All samples display a significant background intensity, suggesting the presence of amorphous carbon. The BC, AC550 and AC650 samples contain graphite-like structures (crystalline carbon), as indicated by the presence of a distinct (002) peak at $22°$ (2θ) and a (100) peak in the vicinity of the graphite (100) at $43°$ (2θ). Similar peaks were reported by Li *et al.*[38] Biochar is often composed of amorphous carbon and may contain traces of other elements depending on its source and formation process. BC550 and BC650, however are a porous form of carbon with a large surface area, resulting from an activation process that may involve thermal and chemical treatments. Fig. 4b illustrates the deconvolution of the BC diffraction pattern using a Gaussian function, revealing two main components (peak 1 and peak 2). The fit quality ($R^2 = 0.93$) indicates a strong correlation with the Gaussian model. In Fig. 4c, the deconvolution of the AC550 sample's diffraction pattern shows increased peak widths and slight shifts in peak positions compared to the BC sample. The R^2 value of 0.77 suggests that this fit is less robust than that of the BC sample, potentially due

to heightened structural disorder. The increased peak widths ($w1 = 6.82°$ and $w2 = 3.70°$) signify structural disorder resulting from the 550 °C thermal treatment. The deconvolution of the AC650 diffraction pattern also displays two main fitted peaks, with peak widths further increased relative to the BC and AC550 samples (Fig. 4d). The R^2 value of 0.54 is the lowest among the three samples, indicating a poorer Gaussian fit, likely due to greater structural disorder. The quality of the Gaussian fit (R^2) decreases as the treatment temperature increases, suggesting that the complexity of the structure in thermally treated samples rises. Additionally, BET data indicate that thermal treatment at 550 °C and 650 °C enhanced the porosity of the samples, which is directly linked to the increased surface area. This increase in porosity may contribute to the observed structural disorder in the treated samples, as evidenced by the XRD analyses.

Thermogravimetry analysis (TGA) of BC, ABC550 and ABC650 adsorbent materials (Fig. 5) was carried out to investigate the stability of the biochar. For both BC and ABC550, the thermogram displays two stages of mass loss. In the BC sample (Fig. 5a), the first stage results in a 5.7% mass loss relative to the total weight, occurring between 30 and 50 °C, primarily due to moisture content. This is typical as water is evaporated from the material when it is heated. The second stage, near 630 °C,
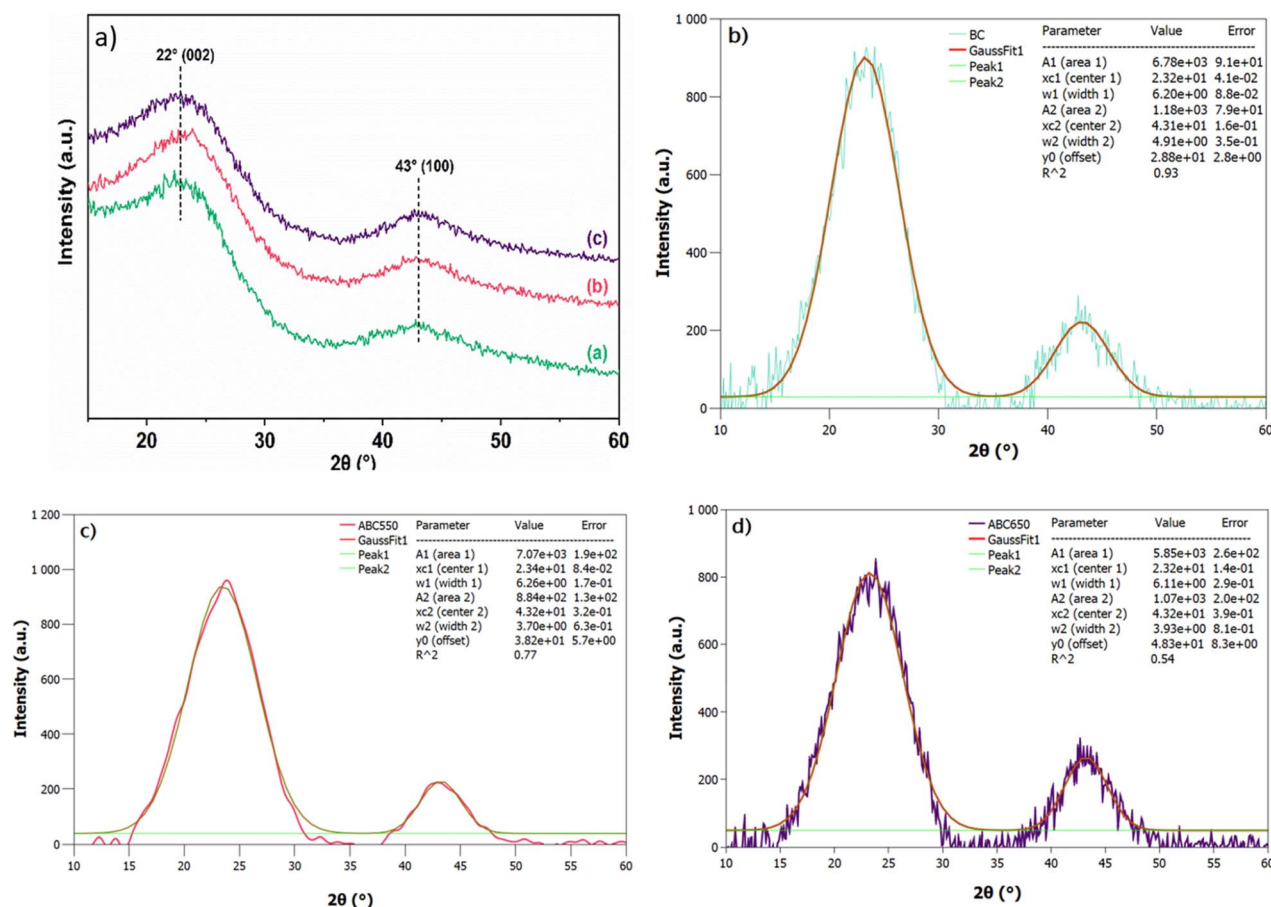

Fig. 4 (a) XRD patterns for (a) BC, (b) ABC550 and (c) ABC650; Gaussian deconvolution of (b) BC, (c) ABC550, (d) ABC650 XRD diffraction patterns with main peaks fitted. The corresponding fitting parameters are listed, including peak positions, widths, and goodness-of-fit (R^2) values.
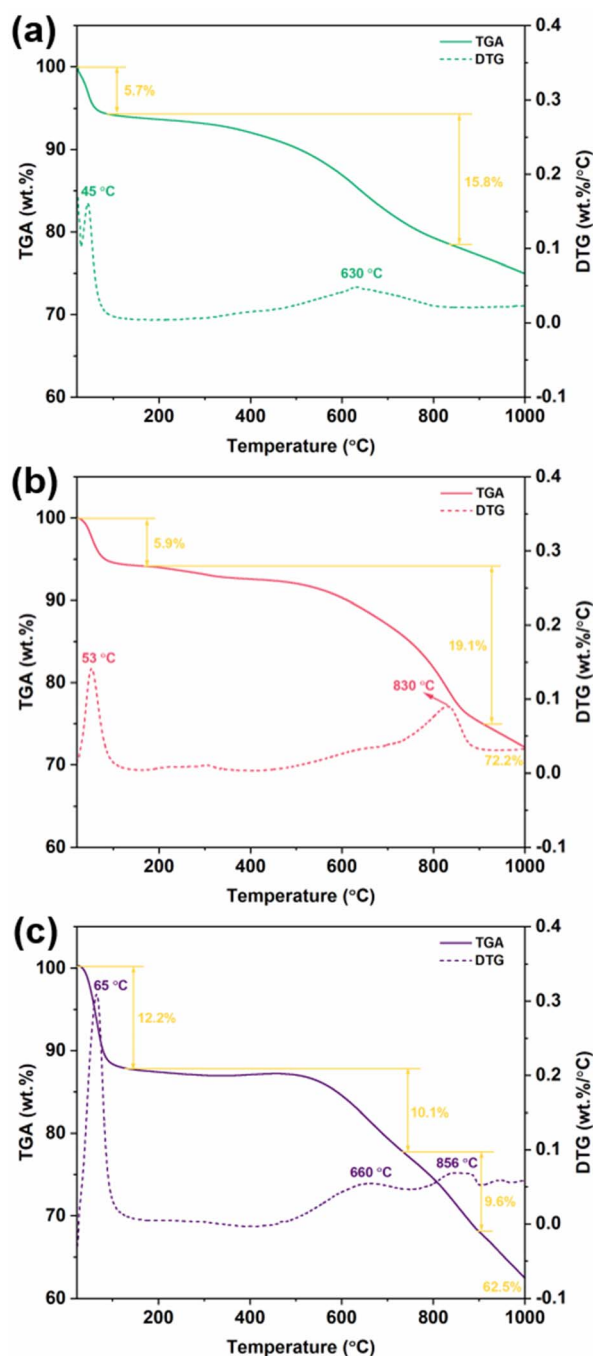
Fig. 5 Thermogravimetry analysis (TGA, solid lines) and derivative thermogravimetry (DTG, dashed lines) curves of (a) BC, (b) ABC550, and (c) ABC650 biochar materials.

accounts for a 15.8% mass loss, attributed release of volatiles, such as gases and organic liquids, present in the carbon. This decomposition can occur over a wider range of temperatures, depending on the type and quality of the carbon.

In the ABC550 sample (Fig. 5b), the first stage shows a 5.9% mass loss at 53 °C, also due to loss of moisture content. The second stage, occurring around 830 °C, results in a 19.1% mass loss due to the elimination of various carbonaceous components.[39] The DTG peak centred at 830 °C may indicate thermal

decomposition of aliphatic C–H structures and a high substitution degree of aromatic rings by oxygen groups.

For the ABC650 sample (Fig. 5c), three stages of mass loss are observed. The first stage, similar to BC and ABC550, occurs at 65 °C with a 12.2% loss. The second stage, at 660 °C, shows a 10.1% mass loss attributed to carbonates.[40] The final stage occurs at 856 °C, with a 9.6% mass loss due to the elimination of various carbonaceous components.

In the TGA analysis, the ABC650 sample exhibited a more significant mass loss compared to ABC550. This observed effect in the sample treated at a higher temperature may suggest enhanced activation of the biochar due to the post-thermal treatment, which could contribute to a further increase in its carbon content and ash composition. Overall, these samples demonstrate expected chemical stability and thermal resistance. The higher fixed carbon content of ABC650 is especially significant, as fixed carbon in biochar generally enhances its stability and resistance to thermal degradation. However, the more substantial mass loss observed in ABC650 may indicate the release of other volatile components or the influence of specific chemical properties that affect its thermal stability.

The morphology of the ABC650 activated biochar was analysed by SEM, as shown in Fig. 6. As it can be observed in Fig. 6a, the material has a fragmented structure with particles of varying sizes. These particles appear to have rough and irregular surfaces, suggesting an activation process that generated a large surface area and porosity. Fig. 6b reveals finer details of the porous structure. The presence of pores of different sizes can be clearly seen, with specific measurements of 4.76 μm and 7.24 μm indicated in the SEM image. This pore distribution is indicative of a highly porous structure, which is typical of activated biochar and is responsible for its high adsorption capacity. These pores can facilitate the capture of molecules of different sizes, making the material effective in various filtration and purification applications.

Aspirin adsorption using *R. ponticum* waste-derived biochars

In this section, the experimental results of aspirin (ASA) adsorption are presented. As previously explained, this drug was selected as a model pharmaceutical compound due to its common presence in contaminated water bodies and easiness in measuring its adsorption characteristics onto carbonaceous materials.

Adsorption isotherms. In the present study, obtained BCs from *R. ponticum* were availed as potential adsorbent materials for the removal of ASA from aqueous solutions. Adsorption isotherms at ambient temperature (25 °C) were obtained for each material and they are presented in Fig. 7.

As evidenced in Fig. 7A, the activating step promoted a significantly increase in the ASA adsorption onto the BC: the inactivated BC presented the lowest adsorbed amount of ASA (113 mg g^{-1}), while ABC550 and ABC650 samples presented the highest values, 267 and 296 mg g^{-1} respectively, which highlights the benefits of activating the material.

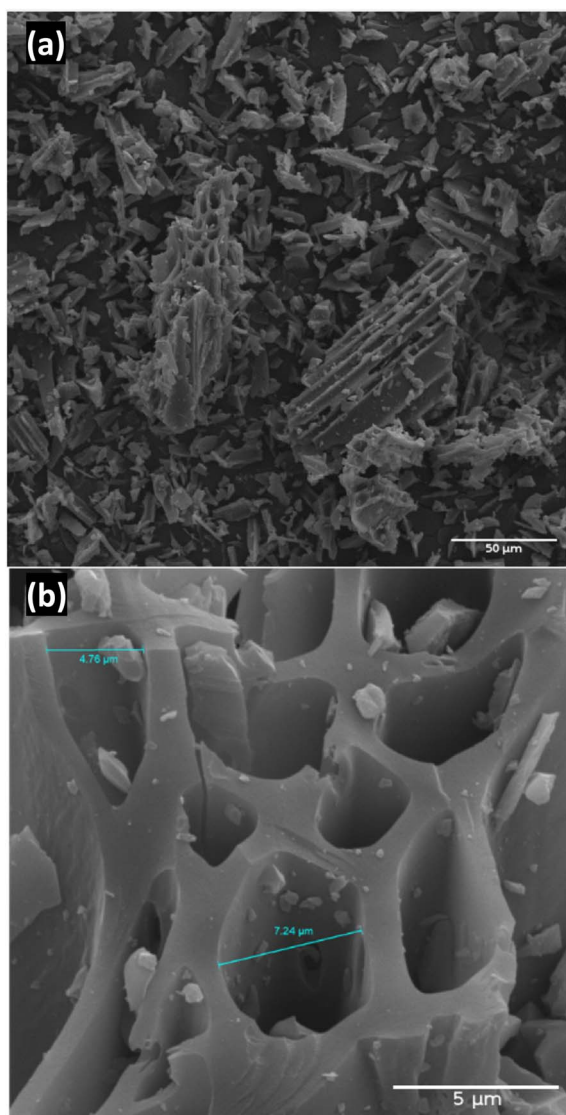When compared to activated biochars obtained from different biomasses, the activated biochar obtained from *R.*

Fig. 6 Morphology of (a) activated biochar produced at 650 °C (ABC650) displayed at a magnification of 1 k and a scale of 50 μm, showing a fragmented structure with irregular and rough surfaces; (b) detailed view of the porous structure of ABC650 sample displayed at a magnification of 10 k and a scale of 5 μm.

Fig. 7 (A) Experimental data and fitted Langmuir's isotherm model of acetylsalicylic acid (ASA) adsorption isotherms at 25 °C onto BC, AB550, and AB650 biochar adsorbents; (B) ASA removal efficiency following adsorption at 25 °C onto BC, AB550, and AB650 biochar materials.

ponticum developed in the current work presents an outstanding performance for ASA adsorption: Wong *et al.*[41] obtained an adsorption capacity of 178.57 mg g^{-1} when using activated biochar derived from spent tea leaves; Mináriková *et al.*[42] evaluated the use of commercial activated charcoal, which presented an adsorption capacity of 218 mg g^{-1}; and Lyyanege *et al.*[43] reported an adsorption capacity of 89.9 mg g^{-1} using Douglas fir biochar.

Higher removal efficiency of acetylsalicylic acid (Fig. 7B) was obtained for lower initial concentrations for the three materials (BC, ABC550, and ABC650), with the highest removal efficiency of almost 90% for ABC650. Such result is of great importance, highlighting that the adsorption of ASA onto the activated biochar from *R. ponticum* is favoured at lower ASA concentrations,
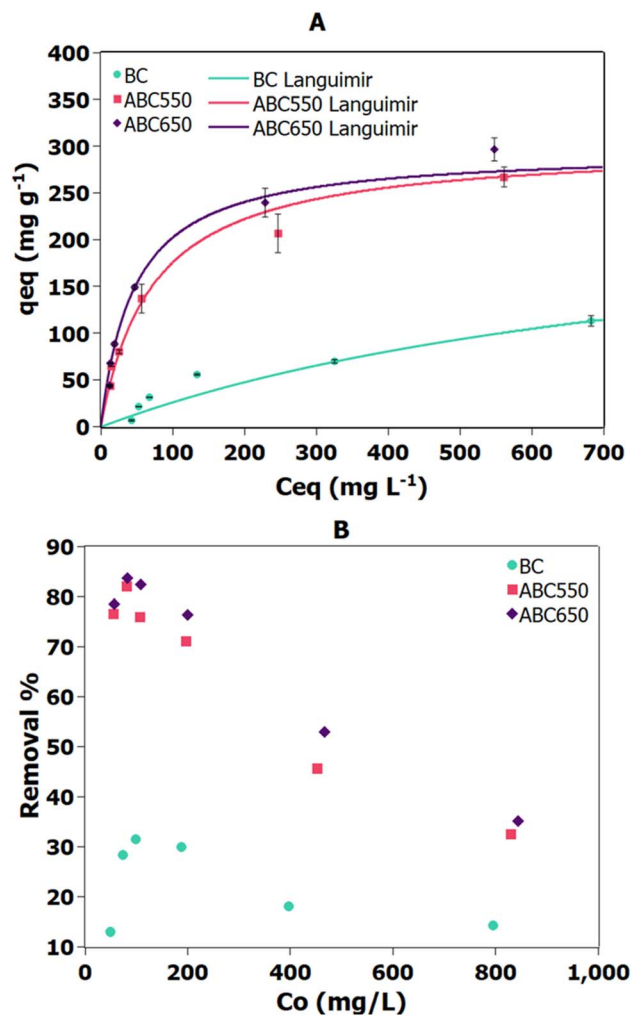
which correspond to the typical contamination levels found in surface water bodies.[43–45]

Modelling of the isotherm data (Table 2) showed that the Langmuir model best described the adsorption onto the activated materials, with very low mean relative errors (MRE = 0.0753 and 0.0924). This suggests monolayer adsorption on a homogeneous surface. The maximum adsorption capacities (q_L) obtained from this model—301 mg g^{-1} for ABC550 and 295 mg g^{-1} for ABC650—are in excellent agreement with the experimental values. In contrast, the inactivated biochar (BC) presented higher relative errors for both evaluated isotherm models (MRE = 0.335 and 0.378), which suggests that the adsorption isotherm of this material must be assessed in a wider range of concentrations for a better fitting result. Fig. 7B, however, highlights that both ABC550 and ABC650 are materials with a higher ASA removal efficiency than BC; hence, the pristine BC material was no further evaluated.

Table 2 Langmuir and Freundlich isotherm model constants and correlation coefficients for the adsorption of aspirin (ASA) onto BC, ABC550 and ABC650 biochar materials[a]

Isotherm model	Parameters	BC	ABC550	ABC650
Langmuir	q_L (mg g^{-1})	261	301	295
	K_L (L g^{-1})	1.11×10^{-3}	1.39×10^{-2}	2.15×10^{-2}
	MRE	0.335	7.53×10^{-2}	9.24×10^{-2}
Freundlich	K_F (L g^{-1})	0.706	21.5	22.2
	$1/n$	0.778	0.403	0.427
	MRE	0.378	0.117	0.163

[a] Parameters: q_L (mg ASA g^{-1} adsorbent) and k_L (L mg^{-1} ASA) are the Langmuir isotherm parameters, and n and k_F (mg$^{(1-1/n)}$ ASA L$^{1/n}$ g^{-1} adsorbent) are the Freundlich isotherm parameters.

When comparing the activated BCs obtained after the thermal treatment at different temperatures, the one activated at 650 °C presented a higher adsorption at the initial concentrations evaluated than the one treated at 550 °C, but there was no significant difference between the fitted values of q_L (301 and 295 mg g^{-1} for ABC550 and ABC650, respectively), suggesting that both the materials present a similar maximum ASA adsorption capacity. The adsorption efficiency shown in Fig. 7B expresses the ratio between the adsorbed amount of ASA and the admitted amount of ASA in the system. For all three materials, the adsorption efficiency was the highest at low initial concentrations, which is a positive result, once ASA contaminations in wastewaters are observed at low concentrations (0.06–0.65 mg L^{-1}).[46–48] Similarly to what was observed for the adsorbed amount (q), the removal efficiency (R) was the highest for the BC activated at 650 °C, followed by the one activated at 550 °C and the inactivated BC.

The use of the *R. ponticum* biomass for the development of activated biochar for the removal of emerging pollutants such as ASA is a prominent alternative for the processing of an invasive plant with no solid waste generation, which enables its use under a circular economy aspect. Beyond this, the sustainability of the industrial production of activated biochar from *R. ponticum* must be assessed, specifically evaluating the economics and environmental aspects such as Life Cycle Assessment (LCA) of the process; however, such analysis falls outside the scope of the present work.

Conclusions

This study successfully demonstrates a circular economy approach by valorising invasive *R. ponticum* biomass into a high-performance activated biochar for removing emerging pharmaceutical contaminants from water. The thermochemical activation with phosphoric acid proved highly effective, drastically enhancing the material's properties. The maximum adsorption capacity for acetylsalicylic acid (ASA) increased by over 160%, from 113 mg g^{-1} for the inactivated biochar to an impressive 295.7 mg g^{-1} for the biochar activated at 650 °C (ABC650). This result, which is well-described by the

Langmuir isotherm model, is highly competitive with other biomass-derived adsorbents. Interestingly, while the ABC650 sample showed slightly superior adsorption, the biochar activated at a lower temperature of 550 °C achieved a nearly identical surface area (876.3 m^2 g^{-1}). This suggests that effective activation can be accomplished under more energy-efficient conditions, further strengthening the sustainability of the process. In conclusion, this research provides a viable pathway to simultaneously manage the ecological threat of an invasive species and address the pressing issue of water pollution. By converting problematic *R. ponticum* waste into a valuable, low-cost adsorbent, this work offers a scalable and sustainable solution for water purification, contributing to the development of green technologies aligned with circular economy principles.

Author contributions

De Lima, T. A. M.: conceptualization, methodology, investigation, data curation, writing – original draft preparation, review & editing. Arantes, M. S. T.: investigation, data curation, writing – review & editing. Araújo, J. A.: investigation, data curation, visualization, writing – review & editing. De Lima, G. G.: conceptualization, visualization, software, writing – review & editing. Andrade, D. M.: methodology, investigation, data curation. Murphy, E. J.: writing – review & editing. Magalhães, W. L. E.: supervision, writing – review & editing. Nugent, M. J. D.: funding acquisition, supervision, writing – review & editing.

Conflicts of interest

There are no conflicts to declare.

Data availability

All data supporting the findings of this study are included in the article. No additional data are available. Additional raw data are available from the corresponding author upon request.

Acknowledgements

References

1 K. H. Hama Aziz, F. S. Mustafa, M. A. H. Karim and S. Hama, *Mater. Adv.*, 2025, **6**, 3433–3454.

2 K. H. H. Aziz, F. S. Mustafa and S. Hama, *Coord. Chem. Rev.*, 2025, **542**, 216875.

3 K. H. Hama Aziz, F. S. Mustafa, M. A. H. Karim and S. Hama, *J. Environ. Manage.*, 2025, **390**, 126245.

4 M. Casati, F. Spicher, T. Kichey and G. Decocq, *Appl. Veg. Sci.*, 2023, **26**, e12734.

5 M. Casati, T. Kichey, D. Closset, F. Spicher and G. Decocq, *For. Ecol. Manag.*, 2023, **549**, 121463.

6 K. Dehnen-Schmutz, C. Perrings and M. Williamson, *J. Environ. Manage.*, 2004, **70**, 323–332.

7 S. Ramangkoon, C. Saenjum and B. Sirithunyalug, *Int. J. Res. Pharm. Sci.*, 2016, **8**, 218–221.

8 S. S. Ningrum and D. Guntama, *AIP Conf. Proc.*, 2022, **2563**, 040011.

9 Y. A. B. Neolaka, Y. Lawa, J. Naat, A. A. P. Riwu, H. Darmokoesoemo, B. A. Widyaningrum, M. Iqbal and H. S. Kusuma, *Environ. Technol. Innov.*, 2021, **24**, 101997.

10 A. Sirimuangjinda, K. Hemra, D. Atong and C. Pechyen, *Key Eng. Mater.*, 2013, **545**, 129–133.

11 F. Oguz Erdogan, *Anal. Lett.*, 2016, **49**, 1079–1090.

12 D. Bosch, J. O. Back, D. Gurtner, S. Giberti, A. Hofmann and A. Bockreis, *Carbon Resour. Convers.*, 2022, **5**, 299–309.

13 S. Lv, L. Ma, X. Shen and H. Tong, *J. Alloys Compd.*, 2022, **906**, 164242.

14 K. H. Hama Aziz, F. S. Mustafa, M. A. Hassan, K. M. Omer and S. Hama, *Desalination*, 2024, **583**, 117725.

15 K. H. Hama Aziz, N. M. Fatah and K. T. Muhammad, *R. Soc. Open Sci.*, 2024, **11**(5), 232033.

16 H. Sütcü, *Biomass Convers. Biorefin.*, 2021, **11**, 1335–1341.

17 H. Sütcü, *Biomass Convers. Biorefin.*, 2021, **11**, 1335–1341.

18 S. Tayibi, F. Monlau, N.-E. Fayoud, E. Abdeljaoued, H. Hannache, Y. Zeroual, A. Oukarroum and A. Barakat, *ACS Omega*, 2021, **6**, 159–171.

19 A. S. Adeleye, J. Xue, Y. Zhao, A. A. Taylor, J. E. Zenobio, Y. Sun, Z. Han, O. A. Salawu and Y. Zhu, *J. Hazard. Mater.*, 2022, **424**, 127284.

20 D. L. S, V. G. B and V. Murali, *Toxicol Rep*, 2024, **13**, 101775.

21 A. H. Nordin, N. Abdul Samad, S. H. Paiman, S. F. Md Noor, A. I. Rushdan and N. Ngadi, *Mater. Today Proc.*, 2024, **96**, 30–34.

22 S. Sharma, R. K. Yadav and A. P. Singh, *Mater. Today Proc.*, 2022, **61**, 1067–1072.

23 B. Ayoubi-Feiz and S. Aber, *Korean J. Chem. Eng.*, 2015, **32**, 2014–2023.

24 M. S. T. Arantes, T. M. P. Miranda, W. L. E. Magalhães, C. V. Helm and V. R. da Silva, *J. Sci. Food Agric.*, 2025, **105**, 132–140.

25 V. H. R. Mongkito, M. Anas, Erniwati, L. O. Rusman and H. Anjanihu, *Int. J. Innovative Technol. Explor. Eng.*, 2020, **9**, 1268–1274.

26 L. Ge, C. Zhao, T. Zhou, S. Chen, Q. Li, X. Wang, D. Shen, Y. Wang and C. Xu, *Energy*, 2023, **267**, 126557.

27 W.-J. Liu, H. Jiang and H.-Q. Yu, *Chem. Rev.*, 2015, **115**, 12251–12285.

28 G. Gündüz, N. Saraçoğlu and D. Aydemir, *Energy Sources, Part A Recovery, Util. Environ. Eff.*, 2016, **38**, 2211–2216.

29 A. Demirbas, *Prog. Energy Combust. Sci.*, 2005, **31**, 171–192.

30 A. Modi, F. Bühler, J. G. Andreasen and F. Haglind, *Renew. Sustain. Energy Rev.*, 2017, **67**, 1047–1064.

31 K. Ravi Kumar, N. V. V. Krishna Chaitanya and N. Sendhil Kumar, *J. Clean. Prod.*, 2021, **282**, 125296.

32 L. Leng, Q. Xiong, L. Yang, H. Li, Y. Zhou, W. Zhang, S. Jiang, H. Li and H. Huang, *Sci. Total Environ.*, 2021, **763**, 144204.

33 I. Širić and J. Falandysz, *Chemosphere*, 2020, **251**, 126614.

34 P.-T. Yeung, P.-Y. Chung, H.-C. Tsang, J. Cheuk-On Tang, G. Yin-Ming Cheng, R. Gambari, C.-H. Chui and K.-H. Lam, *RSC Adv.*, 2014, **4**, 38839.

35 Z. Chen, X. Wang, B. Xue, W. Li, Z. Ding, X. Yang, J. Qiu and Z. Wang, *Carbon*, 2020, **161**, 432–444.

36 N. A. M. Barakat, O. M. Irfan and H. M. Moustafa, *Molecules*, 2022, **28**, 296.

37 B. Sajjadi, T. Zubatiuk, D. Leszczynska, J. Leszczynski and W. Y. Chen, *Rev. Chem. Eng.*, 2019, **35**, 777–815.

38 K. Li, Q. Liu, H. Cheng, M. Hu and S. Zhang, *Spectrochim. Acta, Part A*, 2021, **249**, 119286.

39 M. C. Collivignarelli, W. A. M. A. N. Illankoon, C. Milanese, S. Calatroni, F. M. Caccamo, M. Medina-Llamas, A. Girella and S. Sorlini, *Water*, 2024, **16**, 698.

40 R. R. Nair, M. M. Mondal and D. Weichgrebe, *Biomass Convers. Biorefin.*, 2022, **12**, 4729–4743.

41 S. Wong, Y. Lee, N. Ngadi, I. M. Inuwa and N. B. Mohamed, *Chin. J. Chem. Eng.*, 2018, **26**, 1003–1011.

42 M. Mináriková, V. Fojtikova, E. Vyskočilová, J. Sedláček, M. Šikut, L. Borek-Dohalska, M. Stiborová and M. Martinková, *Environ. Toxicol. Pharmacol.*, 2017, **52**, 214–220.

43 A. S. Liyanage, S. Canaday, C. U. Pittman and T. Mlsna, *Chemosphere*, 2020, **258**, 127336.

44 F. F. Sodré, C. C. Montagner, M. A. F. Locatelli and W. F. Jardim, *Ecotoxicol. Environ. Contam.*, 2007, **2**, 187–196.

45 A. Satayeva, T. Kerim, A. Kamal, J. Issayev, V. Inglezakis, J. Kim and E. Arkhangelsky, *IOP Conf. Ser. Earth Environ. Sci.*, 2022, **1123**, 012067.

46 F. O. Agunbiade and B. Moodley, *Environ. Toxicol. Chem.*, 2016, **35**, 36–46.

47 Z. Moghiseh, A. Rezaee, F. Ghanati and A. Esrafili, *Chemosphere*, 2019, **232**, 35–44.

48 Y. Praveenkumarreddy, K. Vimalkumar, B. R. Ramaswamy, V. Kumar, R. K. Singhal, H. Basu, C. M. Gopal, K. E. Vandana, K. Bhat, H. N. Udayashankar and K. Balakrishna, *Emerging Contam.*, 2021, **7**, 43–51.